

INCLUSIVE PRODUCTION OF NEUTRAL MESONS IN ALICE*

ADAM MATYJA

for the ALICE Collaboration

SUBATECH, Ecole des Mines de Nantes, Université de Nantes, CNRS/IN2P3
Nantes, France

(Received May 25, 2011)

Both π^0 and η neutral mesons have been measured by the ALICE experiment at LHC. These results have been obtained via two photon decay measurement, using the two electro-magnetic calorimeters (PHOS and EMCal), as well as via photon conversion in the central tracking system, CTS. We present preliminary π^0 transverse momentum spectra obtained with PHOS and CTS, measured in proton–proton collisions at $\sqrt{s} = 900$ GeV and $\sqrt{s} = 7$ TeV. Results obtained in PHOS and in the CTS are consistent. We also report on the η/π^0 ratio at $\sqrt{s} = 7$ TeV. Also we compare our experimental π^0 p_T spectra with NLO pQCD theoretical predictions.

DOI:10.5506/APhysPolB.42.1517

PACS numbers: 13.75.Cs

1. Introduction

In 2009–2010, the Large Hadron Collider [1] (LHC) started delivering proton–proton (pp) and lead–lead (Pb–Pb) collisions at the highest energies achieved ever. Protons were collided at center of mass energies up to $\sqrt{s} = 7$ TeV and heavy ions (HI) at $\sqrt{s_{NN}} = 2.76$ TeV, *i.e.*, energies 3.5 and 10 fold larger than at existing colliders like Tevatron and RHIC¹, respectively.

ALICE, a general purpose heavy ion experiment [2] has been designed to conduct researches on a deconfined state of matter, the so-called quark-gluon plasma (QGP). During this starting period of LHC operation ALICE has collected $\sim 9 \times 10^6$ pp minimum bias (MB) events at $\sqrt{s} = 0.9$ TeV,

* Presented at the Cracow Epiphany Conference on the First Year of the LHC, Cracow, Poland, January 10–12, 2011.

¹ The highest energy of Tevatron for pp collisions is $\sqrt{s} = 1.96$ TeV. Collisions of gold heavy ions were carried at RHIC with $\sqrt{s_{NN}} = 200$ GeV.

$\sim 8 \times 10^8$ pp MB events at $\sqrt{s} = 7$ TeV and $\sim 1.7 \times 10^6$ Pb–Pb MB events at $\sqrt{s_{NN}} = 2.76$ TeV. It opens a new era for physics measurements both in pp and in HI collisions with ALICE studying the QGP and its manifestations in a new energy regime.

The study of the π^0 and η neutral meson production spectra presents several interests. First of all, the measurement of their production spectra at high transverse momentum ($p_T \gg \Lambda_{\text{QCD}} = 0.2$ GeV/ c) in hadronic interactions is a valuable testing ground of the perturbative regime of Quantum Chromodynamics (pQCD). Moreover, the behavior of parton–parton interactions at high momentum transfer, called hard processes, is well described by pQCD.

Many measurements of production yields of high transverse momentum π^0 mesons have been carried out in the last years in both pp and $p\bar{p}$ collisions spanning center of mass energies from 20 to 2000 GeV. The agreement between experimental cross-sections and theoretical predictions is good over several orders of magnitude. With the new data collected at the LHC, the neutral meson spectra will be compared with pQCD predictions at an energy never explored before.

In addition, the knowledge of the neutral meson production spectra is essential to extract the direct photon spectrum. Photons which come from π^0 and η meson decays constitute a significant background to the direct photon spectrum. Indeed, in the high p_T region, there are between 10 and 100 times more π^0 than prompt photons. A full control of the π^0 and η production is thus essential to be able to extract the direct photon spectrum.

The study of the neutral mesons spectra in pp collisions is also of interest for heavy ion physics. As a matter of fact, they provide a baseline reference to study their production rates in nucleus–nucleus collisions and especially their evolution as a function of p_T . In the case, when a hot and dense medium is expected to be created, one expects the particle production rate *versus* p_T to be modified due to the jet quenching phenomenon. The effect was observed for the first time at RHIC [3]. A comparison between pp and HI neutral meson production spectra allows to extract the nuclear modification factor, R_{AA} , of π^0 and η mesons [4]. In the PHENIX experiment, the suppression of the π^0 meson production was observed in Au–Au collisions at $\sqrt{s_{NN}} = 200$ GeV in a wide p_T range up to 20 GeV/ c . With the ALICE experiment, we expect to extend the p_T region of study to 30 GeV/ c at the center of mass energy of $\sqrt{s_{NN}} = 5.5$ TeV.

Precise observations of the features of the hot and dense medium at the highest possible energy are very important to determine QGP production phenomena. The models available to describe the behavior and properties of the dense matter were adjusted to available experimental data from SPS to RHIC and extrapolation to the new energy regime was burdened with a

significant error [5]. The information from the LHC experiments will put constraints to parameters (like transport coefficient of quark–gluon matter or initial gluon density) of these models [5].

The paper is organized the following way. The experimental setup with description of the three major subsystems used in the current analysis is introduced in Section 2. The data sample together with the event selection are described in Section 3. Section 4 is devoted to the calibration of the two ALICE calorimeters. The analysis details of π^0 and η meson reconstruction are presented in Section 5. In Section 6 we present the experimental results and the comparison with NLO pQCD calculations. Finally, we conclude in Section 7.

2. Experimental setup

The π^0 and η mesons are detected via their two photon decays. Two different methods for meson reconstruction via invariant mass were tested and applied in this analysis. The first one is based on the direct measurement of the two gammas which are registered in one of the two ALICE calorimeters, the Photon Spectrometer (PHOS) or the Electro-Magnetic Calorimeter (EMCal). The other relies on the indirect reconstruction of photons which first convert in the Coulomb field of a nucleus into an e^+e^- pair². The products of gamma conversions are registered in the central tracking system (CTS) of ALICE which consists of the silicon Inner Tracking System (ITS) and the Time Projection Chamber (TPC). Both reconstruction methods have their advantages and drawbacks which makes them complementary measurements. The method based on gamma conversions has a relatively low efficiency due to the fact that material budget before the TPC is smaller than ~ 0.11 radiation length X_0 , known with an uncertainty below 6%. However, it is compensated by a high acceptance of the CTS. On the contrary, both ALICE electromagnetic calorimeters have smaller acceptance but high gamma detection efficiency. The number of events coming from these two methods are comparable, but the p_T range probed is complementary. With the CTS, we can go down in transverse momentum, $p_T^{\min} = 0.5$ GeV/ c . However, the possible upper limit in p_T is ~ 7 GeV/ c . Calorimeters can extend the range up to $p_T \approx 25$ GeV/ c with the current statistics.

Below, we briefly describe the characteristics of the detectors used for the π^0 and η analysis. The TPC is a cylindrical gaseous detector [6] of 5 m of a diameter and a length of 5 m. The central electrode with voltage of 100 kV allows to operate with a drift field of 400 V/cm and divides the drift volume (90 m³) in two readout parts. The readout chambers (ROC), installed at the two end-plates of the cylinder are divided into 18 sectors.

² A photon energy must be at least 1.02 MeV so that a pair production became possible.

Each sector consists of an inner and an outer chambers (IROC and OROC, respectively). The readout is based on the multi-wire proportional chamber technique. There are 557568 readout pads with three different sizes allocated on 72 ROCs. The TPC covers the full azimuth angle and a pseudo-rapidity region of $|\eta| < 0.9$.

The ITS is the innermost detector and surrounds the beam pipe [2]. It consists of six cylindrical layers of silicon detectors, located at radii between 3.9 and 43 cm. It covers the pseudo-rapidity range³ of $|\eta| < 0.9$. This subsystem was done in three different technologies. The innermost two layers are pixel detectors (SPD for Silicon Pixel Detector), the intermediate two layers are made in drift technology (SDD for Silicon Drift Detector) and the last two are strip detectors (SSD for Silicon Strip Detector). Together with the TPC, the charge particle p_T resolution of the CTS is about 2%.

The EMCal detector is designed in Shish-kebab technology [7]. It covers 100 degrees in azimuth direction, ϕ . In longitudinal direction, it has ~ 700 cm of length, covering $|\eta| < 0.7$. The detector is segmented into 11520 towers. Each tower is made of 76 lead layers with a longitudinal pitch of 1.44 mm each and 77 scintillator layers with thickness of 1.76 mm each. Each tower has a trapezoidal-shape pointing approximately towards the collision point. Its front face area is 6×6 cm² and height is 24.8 cm. Four towers (2×2) form a module. Each module has a fixed width in the ϕ direction and a tapered width in η direction with an aperture angle of 1.5 degrees. There are 12 modules in the ϕ direction in each strip-module. Each Super Module (SM) is assembled from 24 strip-modules. The whole EMCal comprises 10 Super Modules⁴ which are 430–440 cm far from the interaction point (IP). The available acceptance used for the purpose of the analysis presented in this paper was $|\eta| < 0.7$ and $80^\circ < \phi < 120^\circ$. It corresponds to 4 SM. The amount of the material in front of EMCal counts for 0.8 radiation length X_0 .

PHOS is a high granularity Photon Spectrometer [8]. It is composed of lead tungstate (PbWO₄) crystals of size $2.2 \times 2.2 \times 18$ cm³ each. Its total number of crystals in 5 SM is 17920. The current acceptance of the detector is $|\eta| < 0.13$ and $260^\circ < \phi < 320^\circ$. It corresponds to 3 out of 5 PHOS SM. The designed azimuthal coverage is $\Delta\phi = 100^\circ$. The PHOS detector is located in the bottom position of ALICE in the cradle opposite to the EMCal, at the radius of ~ 460 cm. Due to the layout of the ALICE detector the material budget is smaller than for EMCal and is of 0.2 radiation length X_0 .

³ The first layer has an extended pseudo-rapidity coverage to $|\eta| < 1.98$.

⁴ The whole EMCal is available since January 14th, 2011.

3. Data sample and event selection

In 2010, the ALICE experiment has collected samples of proton–proton collisions with the integrated luminosity $\mathcal{L} = 5.5 \text{ nb}^{-1}$ at $\sqrt{s} = 7 \text{ TeV}$ and $\mathcal{L} = 0.14 \text{ nb}^{-1}$ at $\sqrt{s} = 900 \text{ GeV}$. It corresponds to 3.6×10^8 and 6.1×10^6 events, respectively. In the case of the converted gamma analysis, a subsample of $\mathcal{L} = 1.53 \text{ nb}^{-1}$ (10^8 events) with minimum bias trigger at $\sqrt{s} = 7 \text{ TeV}$ has been used [9]. Events with at least one hit in the SPD detector or in the V0 detector are accepted. Further, in the off-line analysis, beam–gas events are suppressed while beam–beam are kept. To remove pileup events, we put constraints on the primary vertex.

4. PHOS and EMCal detector response and calibration

EMCal towers and PHOS crystals are called cells. During the reconstruction procedure the measured signal amplitude in each calorimeter cell is transformed into the energy via some calibration parameters. A proper calibration is necessary to obtain reliable results.

Several neighboring cells form a cluster. Clusters found in PHOS and EMCal are characterized by a position in the global reference frame and a deposited energy. Clusters can be considered as photon candidates.

A brief description of the calibration of the calorimeters is given below. The calibration of central tracking system is described in [2] and [6].

After the PHOS detector installation in the cavern, the high voltage bias of its avalanche photo-diodes (APD) was equalized to provide the same gains, according to the APD data-sheets provided by the constructor. It gave $\sim 20\%$ accuracy. For an improvement of accuracy the collected dataset of proton–proton collisions was used. The improvement is based on the equalization of mean deposited energy in each cell. It allowed to proceed with the relative calibration. The absolute calibration was performed by requiring the measured π^0 mass to give the PDG value [10]. The achieved accuracy of the method is 6.5%.

The EMCal detector was pre-calibrated with cosmic rays in the laboratory. Next, the equalization of the APD gains has been performed as for PHOS. Finally, absolute calibration by adjusting the measured π^0 mass for each cell, to the PDG value was done as for PHOS. Eventually EMCal achieved the accuracy of 7%.

5. Neutral meson reconstruction and analysis

5.1. Reconstruction in calorimeters

In order to proceed with the reconstruction of neutral mesons which decay in two photons, it is necessary to identify which clusters are potentially photon candidates. The main background of these photons comes mostly

from hadrons and minimum ionizing particles. Two simple reconstruction criteria were applied to clusters in calorimeters in order to suppress their contribution: an energy threshold of 0.3 GeV is required as well as at minimum 2 and 3 cells per cluster in EMCAL and PHOS, respectively. The aim of applied requirements is to get rid of clusters with accidental noisy cells. Then, the invariant mass distribution of two clusters, $M_{\gamma\gamma}$, is built from such selected clusters. Examples of π^0 invariant mass spectra reconstructed in different p_T ranges are shown for Fig. 1 for PHOS (left) and EMCAL (right).

In the case of EMCAL, the cluster energy threshold was increased to 0.5 GeV to suppress more background. Examples of invariant mass spectra in the η mass range are shown in Fig. 2 in PHOS (left) and EMCAL (right).

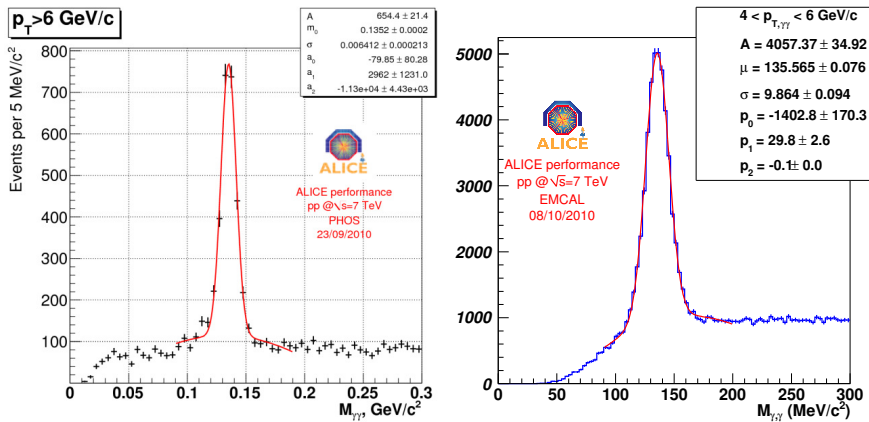


Fig. 1. π^0 invariant mass spectra in PHOS (left) and EMCAL (right).

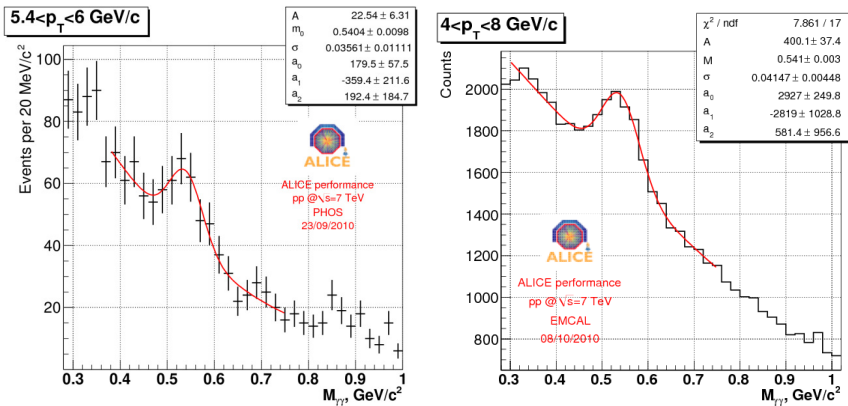


Fig. 2. η invariant mass spectra in PHOS (left) and EMCAL (right).

An additional selection criterion on the photon energy asymmetry, $A = (E_1 - E_2)/(E_1 + E_2)$, has been applied to reduce combinatorial background contribution under the η peak, where $E_{1,2}$ are the energies of the two photons used to reconstruct the η meson. The empirical values of $|A| < 0.7$ and $|A| < 0.6$ have been required in PHOS and EMCal, respectively.

In Figs. 1 and 2, the solid (red) curve denotes fit-line which describes data. Signal has been described by a Gaussian function. A second order polynomial has been used to describe background. Fit parameters are shown in the figures. Peak position and width dependence with p_T are described in the Section 5.3.

5.2. Reconstruction in the CTS

The π^0 and η mesons are reconstructed in the tracking system via the following decays: $\pi^0/\eta \rightarrow \gamma\gamma \rightarrow e^+e^-e^+e^-$. The electron and positron candidates are first selected. The quality requirements for candidates are based on the energy loss, dE/dx , of the charged track together with the rejection of tracks on the pion line in the same dE/dx spectrum. Then, to select photons, two tracks with opposite charges are recombined. They should come from the same vertex with a good χ^2 . The photon mass constraint is applied to that vertex. Moreover, the charged tracks taken into consideration should be parallel to each other at the vertex. The last step is to combine the two reconstructed photons in neutral mesons. The resulting invariant mass of the combined photons for a p_T region larger than 0.4 GeV/c is shown in Fig. 3, where peaks are visible in both π^0 and η mass regions.

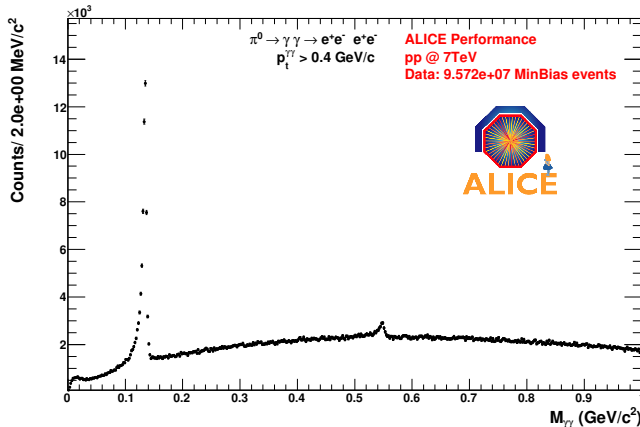


Fig. 3. Invariant mass spectra in the π^0 and η mass range reconstructed in the CTS with the conversion method.

5.3. Analysis

The energy and position resolutions and linearity are basic characteristics of a calorimeter. They affect the distribution of the mean and the width of the reconstructed meson. The dependence of these quantities versus p_T for reconstructed π^0 meson in PHOS, EMCAL and the CTS are shown in Figs. 4, 5 and 6, respectively. The similar analysis was done for η meson, however plots will not be shown in the current paper.

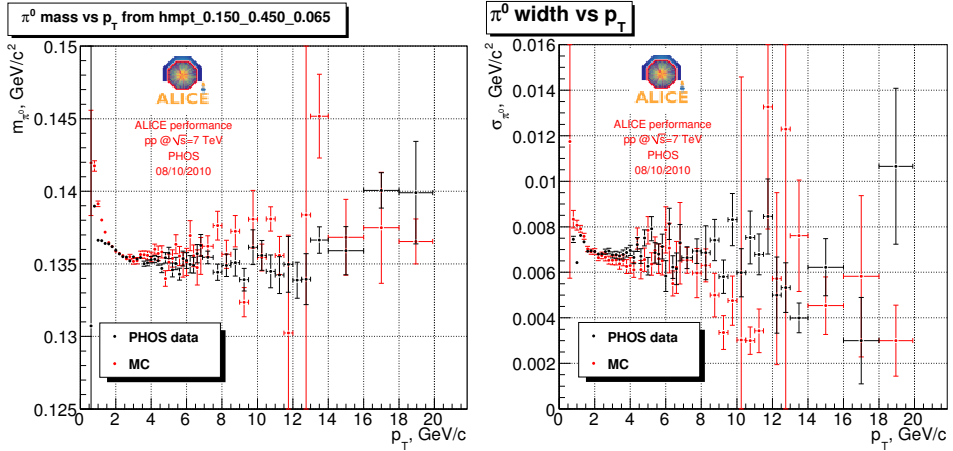


Fig. 4. p_T dependence of the π^0 peak position (left) and width (right) in PHOS.

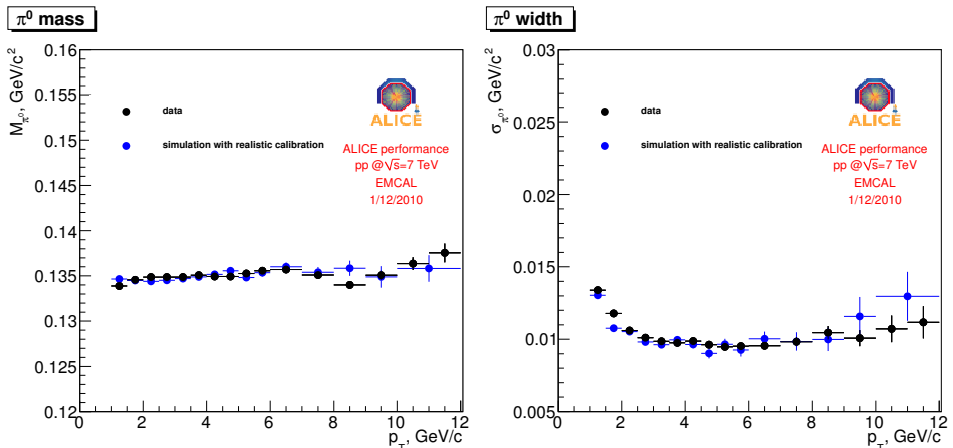


Fig. 5. p_T dependence of the π^0 peak position (left) and width (right) in EMCAL.

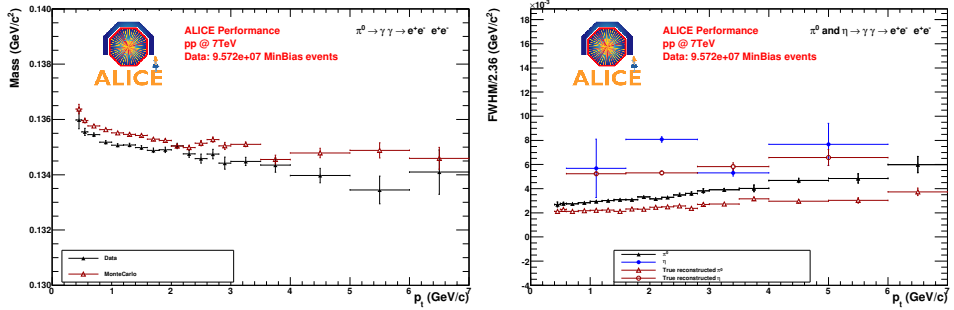


Fig. 6. p_T dependence of the π^0 peak position (left) and width (right) in the CTS.

During data analysis we apply the non-linearity correction taken from test beam [11]. We just note that within error bars, both measured π^0 and η masses are consistent with the PDG values and remain almost constant in a wide p_T range. It means that non-linearity is well known and is under control. In the region of $p_T < 3$ GeV/ c in PHOS, a small increase of mass towards lower p_T values is visible. It is caused by attachment of noisy cells to photon clusters.

Photons coming from π^0 with energy above $E > 6$ GeV tend to merge in EMCal. It has, thus, been necessary to develop a method to separate the overlapping clusters. Knowing the typical shower shape of a single photon cluster we are able to disentangle two (or more) overlapped photon clusters using an unfolding method. According to it one cell can be associated to many clusters. This cell energy is shared between several clusters.

Due to the higher granularity of PHOS, the unfolding is not necessary below the energy of 25 GeV.

The obtained peak width of the π^0 mesons is $\sim 7\%$ within error bars for PHOS and $\sim 10\%$ for EMCal after unfolding and application of other corrections (like nonlinearity correction). It is slightly larger than expected from test beam data with ideal calibration [11]. Due to the residual decalibration of calorimeters the resolution does not achieved the designed value yet. In EMCal, a small rise of the width above $p_T > 10$ GeV/ c is visible due to the inefficiency of unfolding which systematic uncertainty is under study. As shown in the figures 4, 5 and 6, Monte Carlo simulations (by additional 6.5% decalibration of the calorimeters cells) reproduce the behavior of the peak position and the width with p_T . For the η mesons the resolution is $\sim 30\%$ in both calorimeters and seems to decrease a bit with p_T (but it is not shown here).

The width obtained via gamma conversion method is very narrow as shown in the right panel of Fig. 6. It is below 5% for π^0 and below 8% for η in the full p_T range achieved. The smallest width is achieved at lowest momentum, in contrary to the calorimeter cases.

6. Results

To extract meson yields one has to properly subtract the background in the signal window for each p_T range for the invariant mass spectra. The signal window is considered to be within the three standard deviation from the fitted peak mass. The background is mostly combinatorial but in the case of the CTS analysis there is also dalitz contribution. In the case of calorimeters, the invariant mass distribution was parametrized by the superposition of two functions which describe the signal (Gauss) and the background (polynomial). In the case of the CTS, the background which has been estimated by a mixed event technique has first been subtracted from the invariant mass spectra before to fit the remaining distributions with some appropriate fitting functions. A Gaussian function (describing signal) with an exponential and a linear part (possible remaining background) have been combined to estimate the π^0 and η signals under the peaks. The obtained raw spectra were corrected for reconstruction efficiency coming from Monte Carlo simulations. The efficiency grows rapidly up to $p_T \approx 8$ GeV/ c in the calorimeter cases. Then increases a bit up to $p_T \approx 20$ GeV/ c for PHOS reaching 2%. For EMCal the efficiency decreases after reaching the maximum value of $\sim 6.5\%$ around $p_T = 9$ GeV/ c . For the CTS, the efficiency grows up with p_T and reaches an asymptotic value of 0.3%.

The collected data samples allow to measure the π^0 spectrum in pp collisions at $\sqrt{s} = 7$ TeV in the p_T range 0.5–25 GeV/ c with PHOS and from 0.4 to 6 GeV/ c with the CTS via the gamma conversion technique. Due to a smaller data sample the range is limited to 0.4–7 GeV/ c at $\sqrt{s} = 900$ GeV with PHOS. Moreover, the η spectrum at $\sqrt{s} = 7$ TeV is only achievable in the p_T range 0.6–6 GeV/ c in the CTS at that moment, but the range will be increased soon with the other subsystems presented. The invariant π^0 production spectra normalized to the number of pp minimum bias collisions were converted to the differential invariant cross-section of π^0 meson production, $E d^3\sigma/dp^3|_{y=0}$. The total cross-sections of pp collisions $\sigma_{pp} = 50 \pm 10$ mb for $\sqrt{s} = 900$ GeV and $\sigma_{pp} = 67 \pm 10$ mb for $\sqrt{s} = 7$ TeV were assumed for normalization. The obtained production cross-sections together with the Next-to-Leading-Order (NLO) pQCD calculations [12] (with CTEQ5M as the parton density function, KKP as the fragmentation function and for different QCD scales μ) are shown in Fig. 7. The ratio of the measured cross-section to the NLO predictions is shown in the bottom panel of the figures as well. The pink (gray) box represents the pp cross-section uncertainty. We observe that theory describes $\sqrt{s} = 900$ GeV data quite well, while there is a discrepancy between data points and theory at collision energy of $\sqrt{s} = 7$ TeV, even for scale $\mu = 2p_T$.

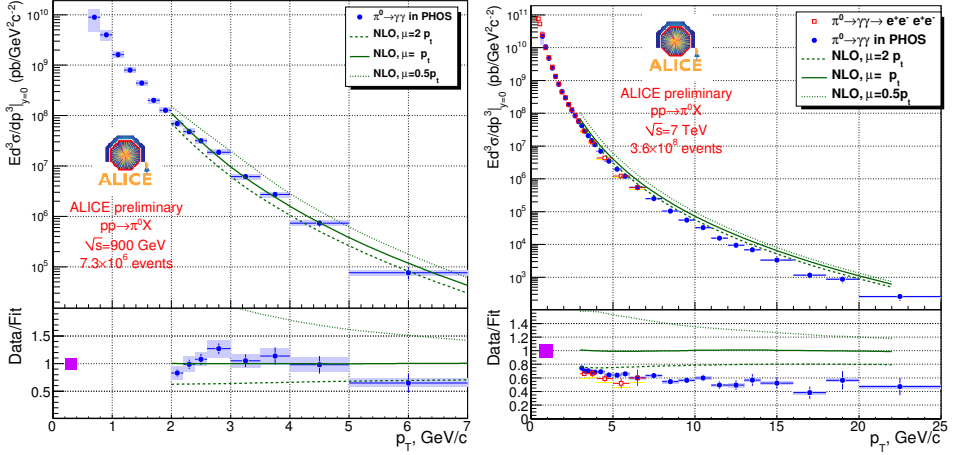


Fig. 7. Differential invariant cross-section of π^0 production in pp collisions at $\sqrt{s} = 900$ GeV (left) and $\sqrt{s} = 7$ TeV (right).

The ratio of η/π^0 production spectra in pp collisions at $\sqrt{s} = 7$ TeV measured in the p_T range 0.6–6 GeV/ c is presented in Fig. 8 for the CTS and compared to PYTHIA predictions and world data measurements. The ratio is in good agreement with both the PYTHIA predictions and the world data measured in hadron–hadron collisions [13].

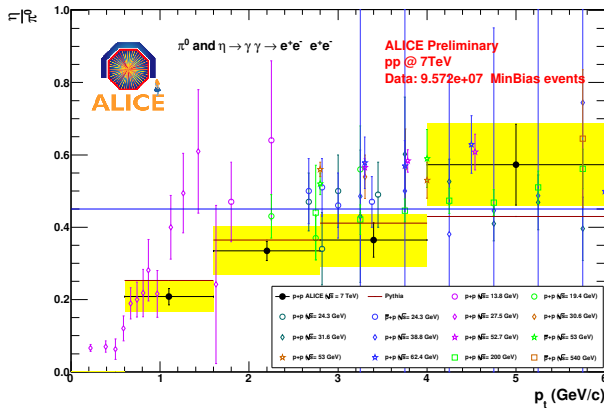


Fig. 8. The p_T distribution of the ratio of η/π^0 production spectra at $\sqrt{s} = 7$ TeV.

The evaluation of systematic uncertainties takes into account different components. The main sources of PHOS measurement uncertainty are absolute energy scale and decalibration, energy non-linearity, geometrical acceptance, raw spectrum extraction, conversion probability and particle identification [14]. In total the systematic uncertainty is 10% above $p_T > 1.5$ GeV/ c . Systematic errors are marked as shadow boxes in Fig. 7.

In the case of the analysis in the CTS, the major contribution to the systematic uncertainty is coming from the material budget. The other sources are signal extraction like: minimum p_T of the electron (e^-) or positron (e^+), requirement on dE/dx of e^\pm , χ^2 of photon reconstruction, track reconstruction in the TPC, energy asymmetry of meson decay products, background calculation and signal integration [15]. The systematic uncertainty depends from p_T and takes values from 5–13%. The smallest uncertainty is in the middle of the distribution and grows towards the edges. Systematic errors are marked as shadow boxes in Figs. 7 and 8.

7. Conclusion

We presented the current status of π^0 and η spectra measurement in the ALICE experiment. The mentioned mesons can be reconstructed from photons registered in calorimeters or via conversion technique. The presented analyses agree with each others. The collected data sample allowed to measure production spectra of π^0 in the p_T range 0.4–7 GeV/ c at $\sqrt{s} = 900$ GeV and 0.4–25 GeV/ c at $\sqrt{s} = 7$ TeV. The η meson spectrum and ratio of η/π^0 were measured in the p_T range 0.6–6 GeV/ c at $\sqrt{s} = 7$ TeV. This range can be extended up to $p_T = 20$ GeV/ c when calorimeters reach the designed resolution. Presented measurements allow to test the pQCD in the hitherto unknown high energy region. The measurements provide also a benchmark for heavy ion collisions.

REFERENCES

- [1] L. Evans, P. Bryant (Eds.), *JINST* **3**, S08002 (2008).
- [2] K. Aamodt *et al.* [ALICE Collaboration], *JINST* **3**, S08002 (2008).
- [3] I. Arsene *et al.* [BRAHMS Collaboration], *Nucl. Phys.* **A757**, 1 (2005);
B.B. Back *et al.* [PHOBOS Collaboration], *Nucl. Phys.* **A757**, 28 (2005);
J. Adams *et al.* [STAR Collaboration], *Nucl. Phys.* **A757**, 102 (2005);
K. Adcox *et al.* [PHENIX Collaboration], *Nucl. Phys.* **A757**, 184 (2005).
- [4] K. Adcox *et al.* [PHENIX Collaboration], *Phys. Rev. Lett.* **88**, 022301 (2002).
- [5] A. Dainese, C. Loizides, G. Paic, *Eur. Phys. J* **C38**, 461 (2005); C. Loizides, *Eur. Phys. J* **C49**, 339 (2007); M. Gyulassy, P. Levai, I. Vitev, *Nucl. Phys.* **B571**, 197 (2000); S. Wicks, W.A. Horowitz, M. Djordjevic, M. Gyulassy, *Nucl. Phys.* **A783**, 493 (2007); S. Wicks, W.A. Horowitz, M. Djordjevic, M. Gyulassy, *Nucl. Phys.* **A784**, 426 (2007); H. Zhang, J.F. Owens, E. Wang, X.-N. Wang, *Phys. Rev. Lett.* **98**, 212301 (2007).
- [6] J. Alme *et al.* [ALICE TPC Collaboration], Ins-Det/10011950 (2010).
- [7] P. Cortese *et al.* [ALICE Collaboration], ALICE EMCAL Technical Proposal, CERN-LHCC-2006-014, CERN-1996-032-Add.3 (2006); [ALICE

- Collaboration], ALICE EMCAL Technical Design Report, CERN-LHCC-2008-014 (2008).
- [8] [ALICE Collaboration], PHOS Technical Design Report, ALICE-DOC-2004-008 v.1.
- [9] K. Aamodt *et al.* [ALICE Collaboration], *Phys. Lett.* **B693**, 53 (2010).
- [10] K. Nakamura *et al.* [Particle Data Group], *J. Phys. G* **37**, 075021 (2010).
- [11] J. Allen *et al.* [ALICE Collaboration], *Nucl. Instrum. Meth.* **A615**, 6 (2010).
- [12] P. Aurenche *et al.*, *Eur. Phys. J.* **C13**, 347 (2000).
- [13] S.S. Adler *et al.* [PHENIX Collaboration], *Phys. Rev.* **C75**, 024909 (2007).
- [14] ALICE Internal Note, Analysis of Inclusive π^0 Production in pp Collisions at $\sqrt{s} = 900$ GeV and 7 TeV Measured with ALICE PHOS, in preparation.
- [15] ALICE Internal Note, Analysis Note: π^0 and η Meson Measurement with Conversions in ALICE in Proton–Proton Collisions at $\sqrt{s} = 7$ TeV and at $\sqrt{s} = 900$ GeV at CERN LHC, in preparation.